

Numerical Simulation of Dynamic Response of Atmospheric Storage Tanks Under Coupling Effect of External Two-source Blast

Junjie Zhu^{1, a}, Mingguang Zhang^{2, b *}

¹ College of Safety Science and Engineering, Nanjing Tech University, Nanjing 211816, China;

² Jiangsu Key Laboratory of Hazardous Chemicals Safety and Control, Nanjing, Jiangsu, 210009, China

^a junjiezhu2021@163.com, ^b mingguang_zhang@njtech.edu.cn

Abstract. In the event of a material leak in an atmospheric steel tank farm, it is likely to cause a fire and explosion, leading to an escalation of secondary accidents. According to the historical domino accident data to analyze the accident characteristics, the explosion phenomenon is common in atmospheric pressure steel storage tank accidents, and the coupling phenomenon is obvious. However, there is a dearth of research on multiple explosions in steel storage tank farms. This paper investigates the dynamic response of an atmospheric pressure storage tank under the coupling effect of simultaneous detonation of two explosive wave sources. With the help of finite element analysis software to establish a simplified model of the tank under the action of two sources of blast wave coupling, to explore the propagation law of the blast wave scenario and the dynamic response process of the tank. The deformation damage of the tanks by the angular size of the blast load is revealed, and the structural energy changes are analyzed. The study of the dynamic response of steel tanks under the dual-source explosion scenario can provide a theoretical reference basis for quantitative damage in realistic scenarios.

Keywords: Explosive load; Numerical simulation; Dynamic response; Atmospheric storage tanks; coupling effect

1. Introduction

Chemical parks have become an important carrier for the high-quality development of China's chemical industry. The layout of the storage tank area in the chemical park is dense, the pipeline facilities are intricate, and the number of substances stored is huge, mostly flammable, explosive, toxic and hazardous substances, which are very prone to domino accidents, as evidenced by serious accidents. On 21 March 2019, a mega-explosion occurred at Tianjiaoyi in Xiangshui, Jiangsu Province, completely destroying the plant. Serious domino accidents have been triggered, causing serious impacts in terms of casualties, property damage and degradation of the surrounding environment. Overseas, Darbra et al. focused on initial accidents that triggered domino accidents by concluding that domino accidents occurred most frequently in the storage tank area (35%), with explosion and fire accounting for 35.5% and 32.5% of the initial accidents, respectively [1]. Similar conclusion was yielded by statistics, explosion and fire, as the main causes of accident extension, accounted for 57% and 43%, respectively [2]. Explosions are a major factor in domino accidents.

Cylindrical thin-shell structures are more widely used in the chemical industry storage applications, for large thin-shell equipment and facilities in the dynamic response under the explosion load and damage mode research is relatively late, storage tanks in the role of the explosion load tend to appear depression, fracture and crushing several damage modes. Explosive experiment has certain limitations, the scientific staff focus on the theory and numerical simulation. Abstraction of empirically based formulas as a means of predicting the explosive power generated by a vapour cloud explosion accident has led to the proposal of the TNT equivalent model, the TNO model, and the Streholw spherical model [3,4,5]. With the popularity and development of computational fluid dynamics methods and computer technology, domestic and foreign researchers

use CFD methods to simulate the process of gas explosion. The finite element model was also developed to investigate the tanks under blast loading [6,7,8,9,10].

The coupling phenomenon in atmospheric storage tank accidents is obvious. This paper investigates the dynamic response of atmospheric storage tanks under the coupling effect of simultaneous detonation of two blast. The study of the dynamic response of steel storage tanks in two blast can provide a theoretical reference basis for quantitative damage in realistic scenarios.

2. Modelling

2.1 Parameters and numerical modelling of atmospheric tanks

According to GB50341-2014 "*Vertical cylindrical steel welded tank design specification*", the tank wall thickness is designed as plotted in Table 1, with the model of $\Phi 21.00 \text{ m} \times H16.58 \text{ m}$.

Table 1. Geometrical parameters of 5000 m³ storage tank

Layer	Thickness/mm	Height/m	Layer	Thickness/mm	Height /m
Bottom	13	-	6th course	8	1.8
1st course	11	1.8	7th course	8	1.8
2nd course	10	1.8	8th course	8	1.8
3rd course	9	1.8	9th course	8	1.8
4th course	8	1.8	Top	6	2.18
5th course	8	1.8	-	-	-

Set the pipeline leakage after the explosion point is located from the ground for 10 m, the distance from the tank for 20 m. Reasonably simulate the propagation of explosive blast waves and completely cover the tank, the air domain shape is selected as a rectangle. As the simulation is a free-field explosion, the boundary selected completely transmissive boundary conditions, according to the above parameters, the use of ABAQUS to establish the external explosion of atmospheric tank explosion analysis model schematic shown in Fig. 1.

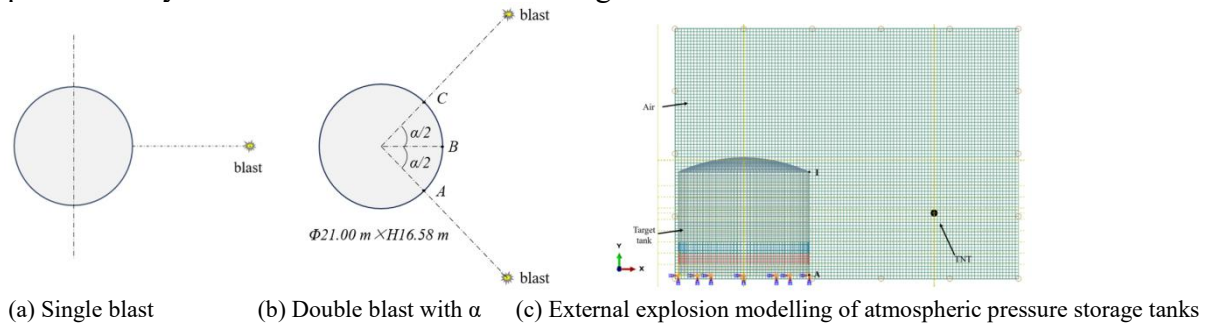


Fig.1 Explosion model of atmospheric storage tank external explosive sources

2.2 TNT explosive equivalent

Explosions that occur in domino accidents are generally vapour cloud explosions. The current construction of the explosion blast wave model is mainly the equivalent conversion of combustible gases into TNT equivalent, TNT equivalent conversion formula as equation (1):

$$W_{TNT} = \frac{\alpha W_f Q_f}{Q_{TNT}} \quad (1)$$

Where: W_{TNT} indicates TNT equivalent, kg; α indicates that the vapour cloud explosion efficiency factor, taking the value of 0.0002~0.159; W_f indicates the total mass of the substance, J/kg; Q_f indicates the heat of combustion of the substance; Q_{TNT} indicates that the heat of combustion of TNT, the general take the value of $4.5 \times 10^6 \text{ J/kg}$.

2.3 Material modelling

2.3.1 Q345 Material Modelling

For simulation purposes, the Mises stress in the fourth strength theory of mechanics of materials is used to determine whether the material enters the plastic state or not. Considering that the material causes high strain rate under explosive loading, the Johnson-Cook empirical model is used in the stress equation to describe the stress-strain of the material, and the expression of the equation is shown below:

$$\sigma = [A + B(\varepsilon^{pl})^n] \left[1 + C \ln \left(\frac{\varepsilon^{pl}}{\varepsilon_0} \right) \right] (1 - T^{*m}) \quad (2)$$

where: σ denotes the rate-dependent yield stress; ε^{pl} denotes the equivalent plastic strain; A , B , m , and n denote the material parameters; and C and ε_0 are the strain-rate hardening index and the reference strain rate, respectively.

In the following equations, ε_f^{pl} denotes the equivalent plastic strain at damage initiation for Q345 steel:

$$\varepsilon_f^{pl} = \left[d_1 + d_2 \exp \left(d_3 \frac{p}{q} \right) \right] \left[1 + d_4 \ln \left(\frac{\varepsilon^{pl}}{\varepsilon_0} \right) \right] (1 + d_5 T) \quad (3)$$

Where: d_1 to d_5 denote the failure parameters; p denotes the compressive stress; q denotes the Mises stress; T denotes the dimensionless temperature parameter.

In this paper, the high-speed strain of the material at room temperature is investigated, and the effect of temperature variation is not involved. The Johnson-Cook model parameters for Q345 steel material are shown in Table 2 below.

Table 2. Q345 steel Johnson Cook parameters.

ρ , kg/m3	E, GPa	ν	A, MPa	B, MPa	C	n	m		
7850	210	0.28	374	795.712	0.01586	0.45451	0.88559		
Melting temp, °C		Transition temp, °C		d1	d2	d3	d4	d5	ε_0
1500		20		0.123	0.236	2.43	0.058	0	1

2.3.2 Modelling of explosive materials

ABAQUS/Explicit was chosen to build the numerical model. Jones-Wilkins-Lee (JWL) equation of state are commonly used to describe the pressure generated by explosion. The JWL equation of state for TNT is expressed as follows:

$$p = A \left(1 - \frac{\omega}{R_1 V} \right) e^{-R_1 V} + B \left(1 - \frac{\omega}{R_2 V} \right) e^{-R_2 V} + \frac{\omega E}{V} \quad (4)$$

Where: p represents the pressure generated at the instant of explosion; V represents the relative volume; E represents the initial internal energy per unit volume of explosives; A , B , R_1 , R_2 , ω are parameters of the JWL equation of state.

The physical parameters of TNT material and the parameters related to the equation of state in JWL are shown in Table 3.

Table 3. Physical parameters of TNT and state coefficients in JWL

Physical parameters		JWL state equation				
ρ , kg/m ³	Detonation velocity, m/s	A, GPa	B, GPa	R1	R2	ω
1690	6930	373.77	3.75	4.14	0.9	0.35

2.3.3 Air material modelling

The air is modelled using the EOS material model, the air is described by the ideal gas equation of state and the state parameters of the air are shown in Table 4.

Table 4. Material parameters of air and state coefficients

ρ , kg/m ³	Atmospheric pressure, kPa	Specific heat capacity, J/(kg·K)	Dynamic viscosity
1.177	101.325	716	1.848×10-5

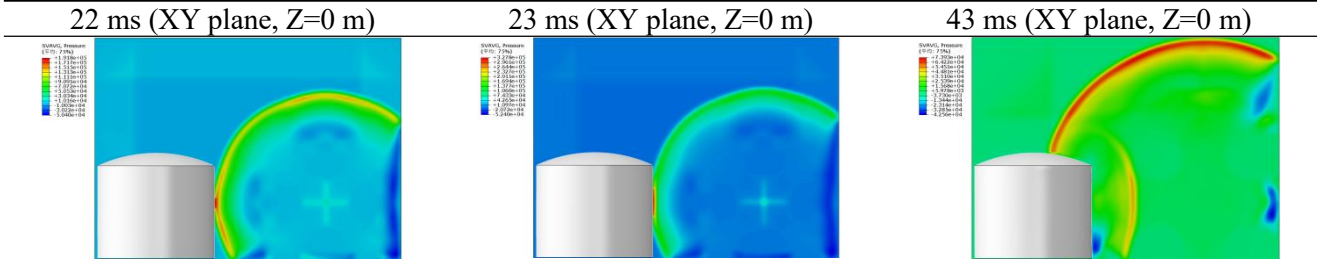
3. Analysis of the results of the tank explosion response

3.1 Blast wave loads and blast wave flow fields

(1) Single blast

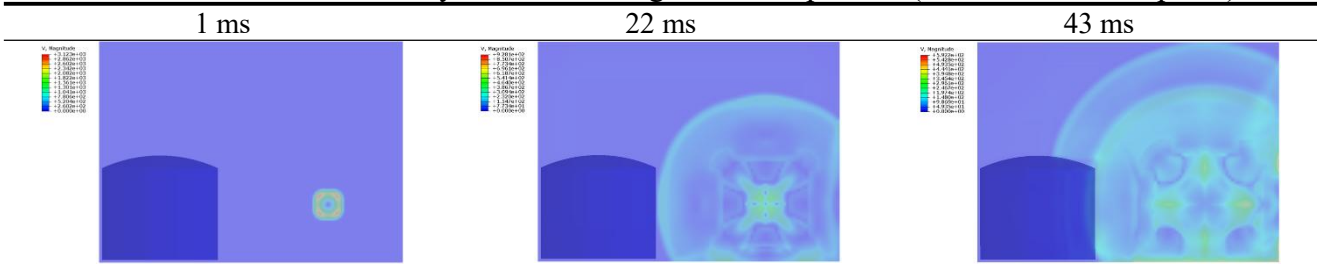
Tank in the external 1000 kg TNT single explosion load, the blast wave overpressure, velocity process is shown in Tables 5-6 below.

Table 5. Peak overpressure contours during the whole process (Front view of XY plane, Z=0 m).



In table 5, blast wave reached the tank at 22 ms, with an overpressure value of 191.8 kPa; at 23 ms, after the interaction with the tank wall contact, a reflected wave was formed, with an overpressure value of 327.8 kPa, and then the overpressure value gradually decreased as it travelled along the ring direction of the tank. Table 6 shows that due to the obstruction of the tank, the explosion front wave speed of 928.1 m/s in 22 ms rapidly decreased to 669.7 m/s in 25 ms.

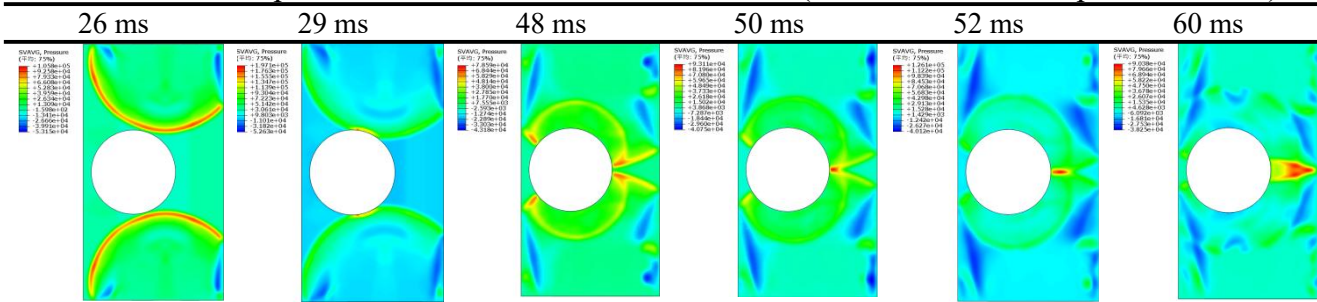
Table 6. Variation of velocity contours during the whole process (Front view of XY plane).



(2) Blast load with 150°

Table 7 shows two equivalent sources and propagation process of blast wave with 150 °. Simultaneous detonation of 26 ms later, the tank wall is the first in the 75 ° and -75 ° direction by the blast damage, and the tank wall in contact with the two peak overpressure of 0.106 MPa. The two equal-source blastwave wavefronts were circumferentially projected around the tank wall, and finally intersected with the coupled blastwave at 0° (Z=0 m) at point B at 52 ms, resulting in a coupled blastwave with a peak overpressure of 0.126 MPa. Subsequently, the blastwave was projected along the wall, and the wavefronts began to decay in terms of the overpressure.

Table 7. Peak overpressure contours with 150° of two blast (Vertical view of XZ plane, Y=10 m).



3.2 Energy changes in storage tank

3.2.1 Tank energy from a single external blast

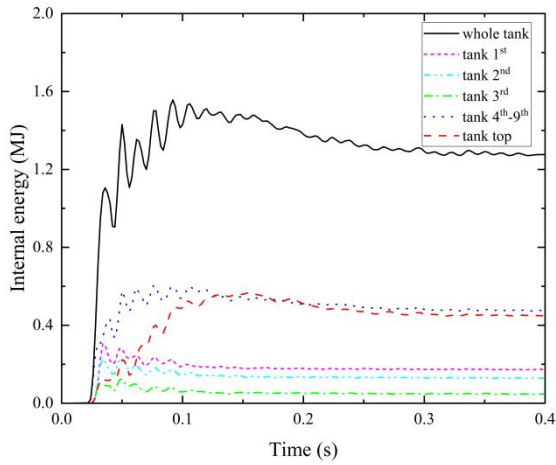


Fig. 2 Time course curves of internal energy for different walls and roof of tank

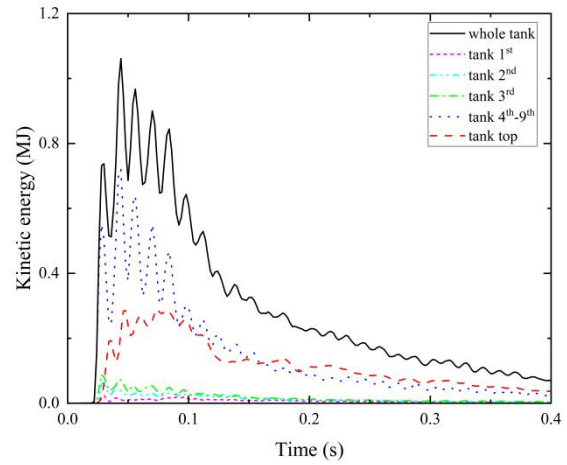


Fig. 3 Kinetic energy time course curves for different tank walls and roof of tank

Figs. 2 - 3 show the tank in a single source of 1000 kg explosion load, the entire tank and the tank wall of the first layer, the second layer, the third layer, the wall of the tank, the top of the internal energy, kinetic energy obtained. 24 ms tank by the explosion blast wave, the entire tank quickly absorbed energy into the structure of the internal energy and kinetic energy, the tank's peak internal energy of 1.56 MJ, the peak of the kinetic energy of 1.06 MJ. The tank's bottom layer is small, not enough to cause the tank to deform. The kinetic energy obtained by the bottom layer of the tank is small, not enough to make the tank deformation, the bottom plate is set as fixed, the first layer has the effect of inhibiting the tank lifting off, the total internal energy is greater than the second layer and the third layer, while the total kinetic energy is the smallest. The maximum internal energy of the upper layer of the tank wall is 0.6 MJ, and the maximum kinetic energy is 0.70 MJ. The maximum internal energy of the top layer of the tank is 0.57 MJ, and the maximum kinetic energy is 0.29 MJ. The internal and kinetic energies acquired by the upper layer of the tank wall continue to increase and are transferred to the roof in a short time, resulting in a rapid increase in the internal and kinetic energies of the roof, which reach the same internal and kinetic energies as those of the upper layer of the tank wall. Tank wall and the top of the circle layer of internal energy, kinetic energy is the largest, the deformation is also the most obvious. After the detonation time of 0.3 s, the tank's internal energy tends to stabilise, the kinetic energy is slowly dissipated state.

3.2.2 Tank energy from external double blast

Figs. 4 - 5 show the internal energy and kinetic energy of the tank in the dual-source explosion load (1000 kg, the angle of 150 °). 26 ms tank by the blast wave, the entire tank rapidly absorbed energy and converted into structural internal energy and kinetic energy, the various parts of the tank wall as well as the vault absorbed internal energy is significantly higher than the kinetic energy. Kinetic energy, the overall internal energy of the tank is mainly in the upper part of the tank wall and the vault, the peak of the tank's internal energy of 4.15 MJ, and the rise slowed down, the total internal energy grows slowly and tends to stabilise, this phenomenon is attributed to the explosion blast wave in a short period of time has not been dissipated, there is a sustained load on the tank wall tank roof, resulting in the continuous absorption of the tank body; the tank's kinetic energy reaches a peak value of 1.51 MJ, with the gradual decay of the course of time. The bottom of the tank ring layer of internal energy, kinetic energy obtained to remain stable, did not undergo a large deformation; the upper part of the tank wall ring layer of the maximum internal energy of 1.34 MJ, the maximum kinetic energy of 0.80 MJ. The maximum internal energy of the top of the tank is 2.62 MJ, the maximum kinetic energy of 0.94 MJ. Compared with the role of a single load, the total internal energy of the tank of the two blast, the total kinetic energy of the tank under the peak significantly increased, respectively, 166%, 42.4%, the increase in total internal energy of the tank

top. Increased by 166%, 42.5%; the total internal energy of the upper part of the tank wall, the total kinetic energy peak increased by 123%, 91.4%; the top of the tank internal energy, kinetic energy peak increased by 360%, 224%. The roof of the explosion loaded by the internal energy, kinetic energy increased rapidly, the energy is greater than the total internal energy of the upper part of the tank wall circle, kinetic energy, the vault region has undergone a more significant plastic deformation, that is, the coupled impact strength more than a single load case.

Figs. 6 - 7 show the internal energy and kinetic energy of the tank in the dual-source explosion load (1000 kg, the angle of 180°). The internal energy of the tank reaches a peak value of 1.74 MJ, showing a slow decline and tend to stabilise; the kinetic energy of the tank reaches 1.11 MJ after the peak shows a rapid decay characteristics. The maximum internal energy of the upper part of the wall layer of 0.74 MJ, the maximum kinetic energy of 0.76 MJ. The maximum internal energy of the roof structure of 0.98 MJ, the maximum kinetic energy of 0.52 MJ. Compared with a single case of explosive load, tanks under the explosion load of 180° , peak of the total internal energy, the total kinetic energy have a significant increase in the increase of 11.5%, respectively, 4.7%. The total internal energy of the upper part of the wall, the total kinetic energy, the total internal energy, the total kinetic energy and the total kinetic energy, respectively, increased by 11.5%, 4.7%. The total internal energy and total kinetic energy of the upper part of the wall increased by 23.3% and 8.6%, respectively. The top of the tank internal energy and kinetic energy of the peak value of the increase is more significant, reaching 71.9% and 79.3%, respectively.

The results show that under the action of dual-source explosion load, the energy response of the tank structure is significantly enhanced, especially in the roof area, the concentration and release of energy is more intense, this phenomenon for the explosion-resistant design and safety assessment of the tank structure is of great significance as a guide.

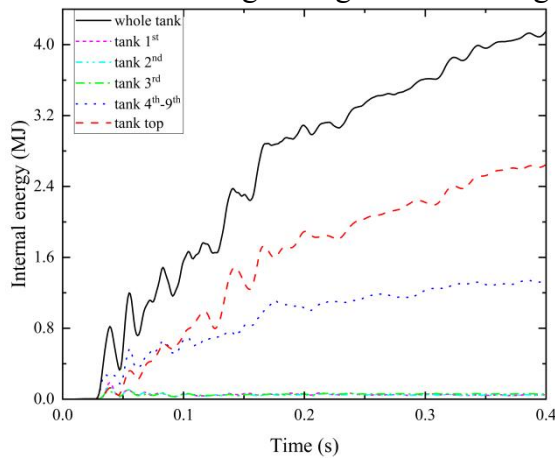


Fig. 4 Time-course curves of internal energy of tanks under 150° explosive loading

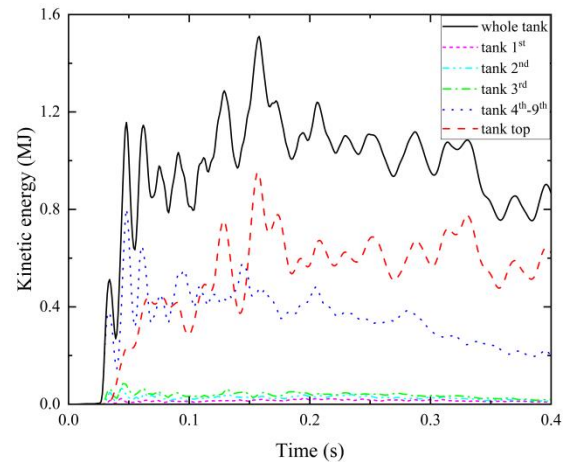


Fig. 5 Kinetic energy time-course curves of the tanks under 150° explosion loading

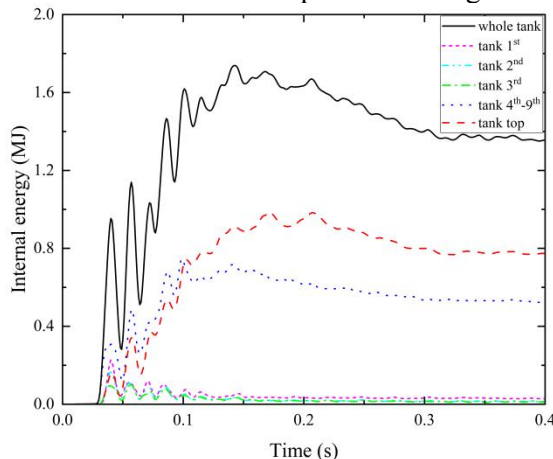


Fig. 6 Time-course curve of internal energy of the tank under 180° explosive load

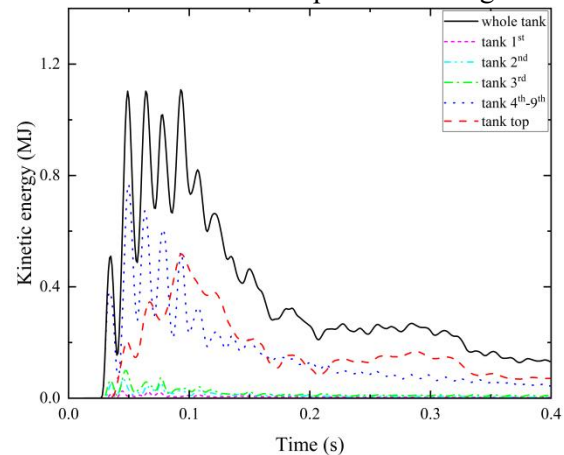
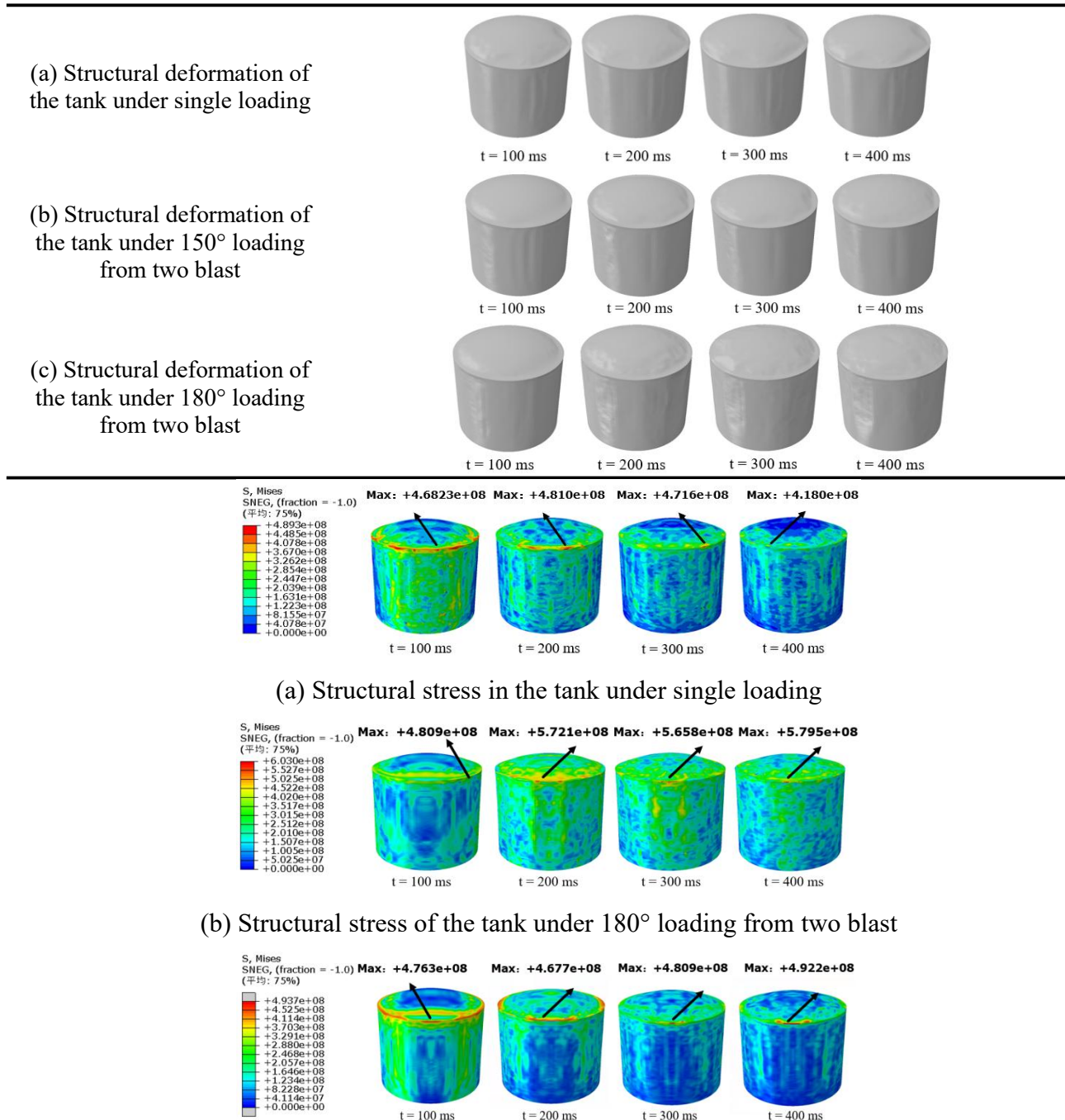


Fig. 7 Time-course curve of kinetic energy of the tank under 180° explosive load

3.3 Structural deformation and stress in storage tanks

Table 8 shows the TNT-equivalent mass of single blast and two blast of different angle loading under the structural deformation of the tank, the tank to the explosion surface and connected to the roof of the tank part of the larger deformation; 200 ms, tank deformation reached a maximum of two blast coupled to the impact of the tank under the deformation of the tank is greater than a single blast, 150 ° in the study under the clamping angle of the load produced by the tank on both sides of the deformation of the larger. Fig. 9 shows the TNT equivalent mass of single-explosive sources and two explosive sources of different angle loads under the structural stress of the tank, the tank wall and the roof of the tank produced the greatest stress, coupled with the angle of the tank generated by the structural stress is greater than in the case of single-explosive sources of the study of 150 ° angle of the load generated by the greatest stress. The smaller the angle of action to the tank of the impact load is greater.

Table 8 Structural deformation of the tank



(c) Structural stress of the tank under 180° loading from two blast

Fig. 9 Structural stress in the tank

4. Summary

The dynamic response of an atmospheric steel tank under two sources of explosive loading was analyzed using the finite element method of ABAQUS. The following conclusions were drawn.

The structural stresses in steel atmospheric tanks under two-source explosive loading are smaller than those generated by single explosive loading, and the tanks are subjected to greater coupled-action loading. Compared with a single explosive source, in 150 ° explosion load, peak of the total internal energy and total kinetic energy in the tank significantly increased, respectively, increased by 166%, 42.5%; peak of the total internal energy and the total kinetic energy in tank wall increased by 123%, 91.4%; peak of the internal energy and the kinetic energy in tank top increased by 360%, 224%. 180 ° explosion load tank total internal energy, the total kinetic energy of the tank's peak, respectively Increased by 11.5%, 4.7%; peak of the internal energy and kinetic energy in tank increased significantly, respectively, reached 71.9%, 79.3%. The energy absorbed and transformed by the tank under the clamp load is larger, and the deformation is more serious.

Acknowledgements

The authors thank the National Natural Science Foundation of China (71971110), the 2023 Key Research Plan (Social development) in Jiangsu Province (BE2023809) and the key project of National Natural Science Foundation of China (51834007) for their financial support.

Reference

- [1] Darbra R M, Palacios A, Casal J. Domino effect in chemical accidents: Main features and accident sequences. *Journal of Hazardous Materials*, 2010, 183(1-3): 565-573.
- [2] Abdolhamidzadeh B, Abbasi T, Rashtchian D, et al. A new method for assessing domino effect in chemical process industry. *Journal of Hazardous Materials*, 2010, 182(1-3):416-426.
- [3] Beshara F B A. Modelling of blast loading on aboveground structures-I. General phenomenology and external blast. *Computers & Structures*, 1994, 51(5):585. 596.
- [4] Wiekeam B.J. Vapor Cloud Explosion Model. *Journal of Hazardous Materials*, 1980, 3:221-232.
- [5] Strehlow R.A., Luckritz R.T., Adamczyk A.A., Shimpi S.A. The blast wave generated by spherical flames. *Combustion and Flame*, 1979, 35.
- [6] Zhang, B.Y., Li, H.H., Wang, W., 2015. Numerical study of dynamic response and failure analysis of spherical storage tanks under external blast loading. *J. Loss Prev. Process. Ind.* 34, 209–217.
- [7] Pan X, Xu J, Jiang J. Simulation analysis of dynamic response of thin-wall cylindrical tank to blast wave. *JOURNAL OF CHEMICAL INDUSTRY AND ENGINEERING-CHINA-*, 2008, 59(3): 796.
- [8] Lu S.Z., Chen W.D., Wang W., Zhang W.S. Numerical simulation on the dynamic response of fixed-roof oil storage tank under the effect of blast loading. *Oil & Gas Storage and Transportation*, 2018, 37(06):644-650.
- [9] Hu G, Fei X, Li J. The transient responses of two-layered cylindrical shells attacked by underwater explosive blast waves. *Composite Structures*, 2010, 92(7):1551-1560.
- [10] Hu K, Zhao Y, Wang Z. CFD simulation of internal flammable gas explosion loading in core-roof steel tanks. *J. Vib. Blast*, 2015, 34(12): 150-156.